

## DIGITAL TERRAIN ANALYSIS OF THE DYNAMIC WETNESS PATTERN ON THE SULMACHUN WATERSHED

S. Kim\* and S. Jung\*\*

\* *Department of Environmental Engineering, Pusan National University,  
San 30, Jangjungdong, Gumjunggu, Pusan, Republic of Korea, 609-735 (E-mail: kimsangh@pnu.edu)*

\*\* *Korea Institute of Construction Technology, Koyang city,  
Kyongkido, Republic of Korea, 411-712 (E-mail: swjung@kict.re.kr)*

### ABSTRACT

Formulation of the dynamic topographic wetness index was extended from the quasi-dynamic wetness index to predict the spatial and temporal distributions of the water and pollutant movement patterns and soil moisture. An algorithm of the dynamic wetness index was developed through integrating the convolution integral of the up-slope area with the time series of effective rainfall. The spatial and temporal behaviors of the dynamic topographic wetness index of the Sulmachun Watershed, located in the northern area of Seoul, were calculated using the digital elevation model (DEM) and rainfall data. The spatial distribution of the dynamic wetness index shows most the diffusive feature of flow generation among the three assumptions of the steady state, quasi-dynamic and fully dynamic algorithms. The spatial distribution of the quasi-dynamic wetness index and of the dynamic wetness index approximate that of the steady state wetness index as the time step is increased. The fully dynamic wetness index shows dual peak distributions of the normalized probability density function (PDF) while the other assumptions results appear as a single peak of the PDF. The issue of the resolution of the fully dynamic topographic wetness index has been explored on the platform of the DEM.

**Keywords:** GIS, Catchment Management, Water and Pollutant Movement, Spatial Analysis, Digital Elevation Model

### INTRODUCTION

The spatial and temporal distribution of the water movement pattern at an upland watershed scale is one of the important components in understanding the spatial characteristics the diffusive pollution. The chemical concentration in overland flow is affected by the contact time of an overland flow parcel with the soil surface (Wallach *et al.*, 2001). The spatial distribution of soil moisture significantly impacts runoff mechanisms (Troch and Brutsaert, 1993). The soil moisture conditions were found to be one of principle factors not only in estimating the potential of non-point source pollution (Torbert *et al.*, 1999) but also in improving the simulation of AGNPS (Perrone and Madranootoo, 1999).

Topography plays a dominant role in hydrologic behavior such as soil moisture in a humid, temperate and gentle sloped watershed (Beven and Wood, 1983). The saturation-excess overland flow has been simulated using the topographic wetness index. The relationships between surface soil moisture and topography show the potential of the  $\ln(a/\tan\theta)$  index as an indicator of Digital Elevation Model (DEM) hydrology (Western *et al.*, 1999), even though the steady-state assumption of TOPMODEL that  $a$  is defined as the upslope area per unit contour length and  $\tan\theta$  is the local terrain slope, has been criticized, (Barling *et al.*, 1994; Wigmosta and Lettenmaier, 1999). The causality between water quality parameters and the saturation deficit based on the  $\ln(a/\tan\theta)$  index was explored by Kim and Delleur (2001). In this study, the fully dynamic topographic-based wetness index is developed from the quasi-dynamic topographic wetness index (Barling *et al.*, 1994). The application of the steady topographic index, the quasi-dynamic index and the fully dynamic index will be compared to evaluate the steady state assumption. The characteristics of the quasi-dynamic wetness index and the dynamic wetness index are discussed on the basis of the spatial and statistical aspects depending upon resolutions of the DEM and the drainage time.

### MATERIALS AND METHODS

#### *The Static Wetness Index*

The  $\ln(a/\tan\theta)$  index has been used as a hydrologic surrogate of topography, where  $a$  is the upslope accumulated area and  $\tan\theta$  is the local terrain slope evaluated from the DEM analysis (Beven and Kirkby, 1983; Kim and Delleur 2001). The spatial distribution of water accumulation can be calculated based on the assumption that the local lateral hydraulic gradient can be approximated from the local slope. The single flow direction algorithm (*sfd*) (O'Callaghan and Mark, 1984) allows the flow path to a pixel only in the steepest direction to the eight neighboring pixels. Multiple flow direction algorithms (*mfd*) allocate flow from a pixel to any downslope adjacent pixel by the ratio of a directional slope times the contour length to the summation of eight direction slopes times the contour lengths (Quinn *et al.*, 1991). In this study, *sfd* was selected as the analysis algorithm because we believe that the flow divergence patterns of several assumptions could be properly compared on the platform of *sfd*.

**The Quasi-dynamic Wetness Index**

The effective upslope contributing areas play an important role in determining the distribution of soil water content and the formation of soil saturation zones. Barling et al.(1994) incorporated the concept of time area curves into the platform of the contour-based Topographic Analysis Program for Environmental Science-Grid (TAPES-G) terrain analysis program. The discharge per unit width of contour  $q(t)$  and the depth of saturated throughflow  $h(t)$  to a constant recharge rate  $r_0$  can be expressed as

$$q(t) = r_0 \cdot a(t) \quad (1)$$

$$h(t) = \frac{r_0}{K_s \tan \mathbf{b}} \cdot a(t) \quad (2)$$

where  $K_s$  is the saturated hydraulic conductivity and  $\tan \mathbf{b}$  is the slope of the soil surface. The effective upslope contributing area per unit width of contour for the specific drainage period is

$$a(t) = \sum_{i=1}^n A_i / b \quad (3)$$

where  $n$  is the number of upslope cells and  $A_i$  is the area of element  $i$  contributing to the subsurface drainage. The upslope area can be evaluated as

$$A_i = \int_0^{s_i} b \cdot ds \quad t_{i-1} < t < t_i \quad s_i = \frac{\mathbf{h}(t - t_{i-1})}{K_s \tan \mathbf{b}} \quad (4)$$

$$A_i = A_{ii} \quad t > t_i \quad s_i = s_{i\max} \quad (5)$$

$$A_i = 0 \quad t < t_{i-1} \quad (6)$$

where  $b$  is the cell length of the DEM,  $s_i$  is the flow path for element  $i$ ,  $\mathbf{h}$  is the effective porosity,  $t$  is the drainage and  $t_i$  or  $t_{i-1}$  are the time for all element  $i$  or  $i-1$  contribute to the specific cell, respectively.

**The Dynamic Wetness Index**

Considering the temporal variation of recharge rates and the hydraulic conductivity of the soil matrix, the discharge rate,  $q(t)$ , and the depth of saturated throughflow,  $h(t)$ , can be convoluted as

$$q(t) = \int_0^s \frac{da}{d\mathbf{t}} r(t - \mathbf{t}) d\mathbf{t} \quad (7)$$

$$h(t) = \frac{1}{K_s \tan \mathbf{b}} \int_0^s \frac{da}{d\mathbf{t}} r(t - \mathbf{t}) d\mathbf{t} \quad (8)$$

where  $r(t)$  is the recharge rate at time  $t$  and  $\mathbf{t}$  is the integration variable.

The saturated hydraulic conductivity  $K_s$  can be calculated using the analysis of grain-size composition (Vukovic and Soro, 1992) as

$$K_s = \frac{g}{\mathbf{n}} \cdot C \cdot \mathbf{j}(\mathbf{h}) \cdot d_e^2 \quad (9)$$

where,  $g$  is the gravitational acceleration,  $\mathbf{n}$  is the dynamic viscosity,  $C$  is the value of the coefficient,  $\mathbf{j}(\mathbf{h})$  is the function of porosity and  $d_e$  is the effective grain diameter.

A flowchart of the computation of the dynamic wetness index is shown in Figure 1. The drainage time and the time series of the effective rainfall are used to determine the upslope flow accumulation in the DEM.

**RESULTS AND DISCUSSION**

Sulmachun Creek, located in the headwaters of the Imjin River of northern South Korea, was selected as the study area. The watershed area is 8.5 km<sup>2</sup>, and the channel length is about 5.8 km. The elevation of the catchment ranges from 59 m to 675 m above sea level, with slopes varying from 0 to 50 %. The annual precipitation is about 1,600 mm, and the temperature varies from -10 to 35 degrees Celsius over the year. The topography of the watershed was digitized by using a 1:5,000 scale elevation map from the Korean Geological Agency. A topographical map with a 10 m by 10 m grid with the digitized channel is presented in Figure 2. The rainfall between January 6th of 1999 and April 18th 2001 is shown in Figure 3.

The hydraulic conductivities of the Sulmachun watershed were estimated using equation (9) with soil samples collected from the field. The average of the measured hydraulic conductivities was 2.38 m/day. Depending on the drainage times, the spatial distributions of the dynamic wetness index were calculated as shown in Figure 4. As the drainage time increases from 1,000 hr to 10,000 hr, the saturation tendency appears to be concentrative. The organization of the wetness pattern can be observed in later time steps. Figure 5 compares the spatial distributions of wetness indices associated with various

assumptions such as the steady state, quasi-dynamic and fully dynamic approaches. The diffusive flow pattern appears to be most significant in the fully dynamic wetness index, among the three assumptions. The heterogeneity of temporal rainfall may provide an additional diffusivity to the distribution of the saturation pattern. The distribution ranges of the dynamic index are different from those of other approaches due to the convolution of the actual rainfall data in the computation. However, the spatial distribution of the relative saturation tendency is comparable.

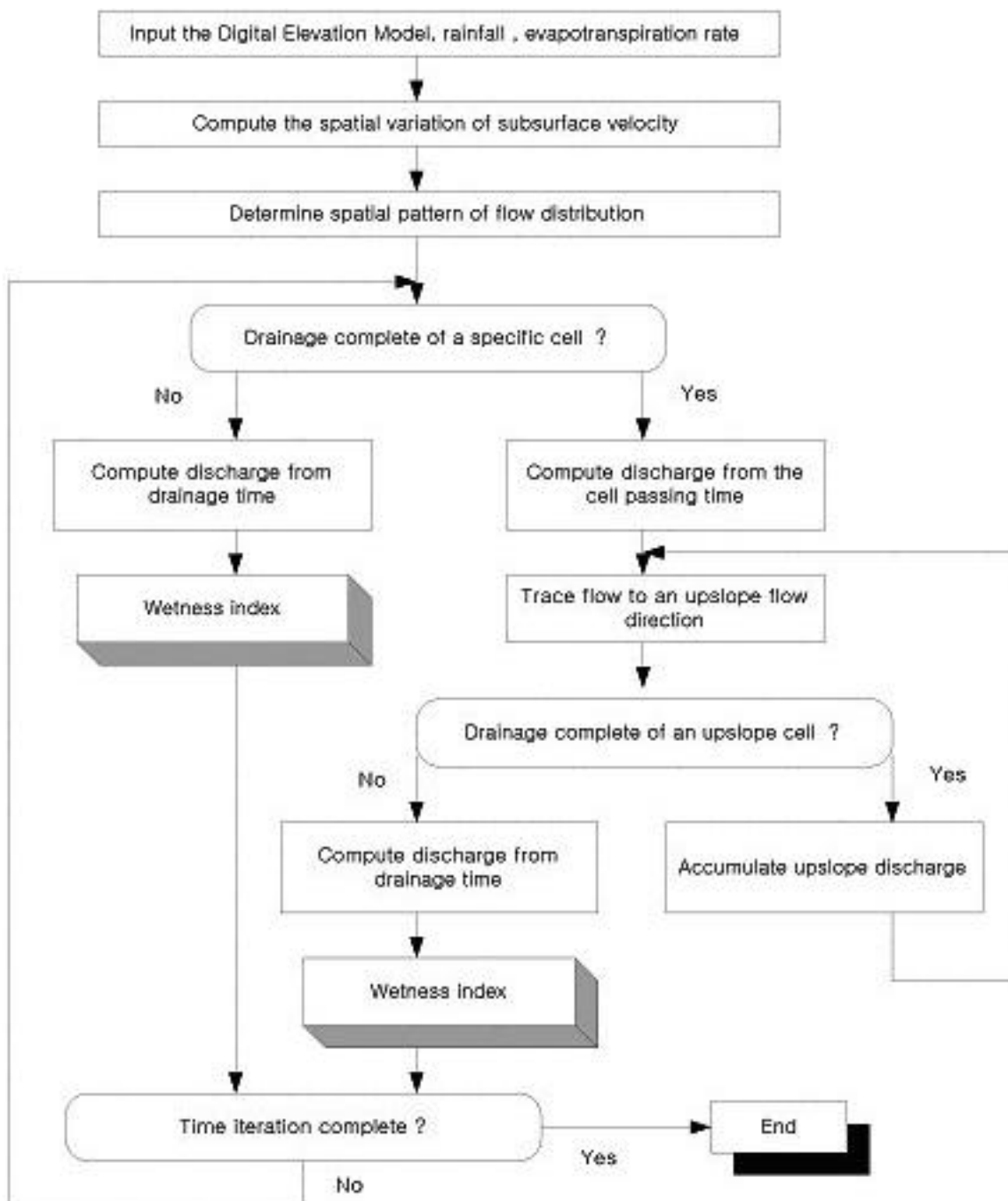


Figure 1. The flowchart of the dynamic wetness index computation

The spatial distributions of the quasi-dynamic wetness index and the dynamic wetness index approximate to the steady state wetness index over time. Figure 6 shows the normalized probability distribution functions of the steady wetness index as well as the dynamic wetness indices for the various drainage times. The distribution of the dynamic wetness index also tends to approximate to the steady state wetness index as over time. The fully dynamic wetness indices show dual peak distributions of the normalized probability density function (PDF) while the other assumptions, results appear as a single peak of the PDF. The temporal variability of rainfall introduces completely a different characteristic of statistical aspect of the saturation tendency. The lower parts of dual peaks are associated with the top of the hill or diverging area of watershed topography.

The resolution issue of the dynamic wetness index has been explored on the platform of DEM. Figure 7 shows the normalized PDFs of the dynamic wetness indices of various resolutions with 20,000 hours of drainage time. The dual distributions of the PDF were found on a pixel size of less than 30 m. Unstable and irregular distributions of the PDF were produced on a resolution greater than 50 m. A pixel size threshold for stable and consistent computation exists between the 30 m and 50 m pixel sizes. The propagation velocity of subsurface flow with the characteristics of rainfall and the size of DEM determine the statistical distribution as well as the spatial distribution. The spatial distribution of flow distribution pattern seems significantly distorted by the rainfall heterogeneity in the pixel size greater than 50 m. The inconsistent distribution of PDF in resolution 50 m, 80 m and 100 m indicates the spatial flow distribution patterns appear different in each pixel sizes.

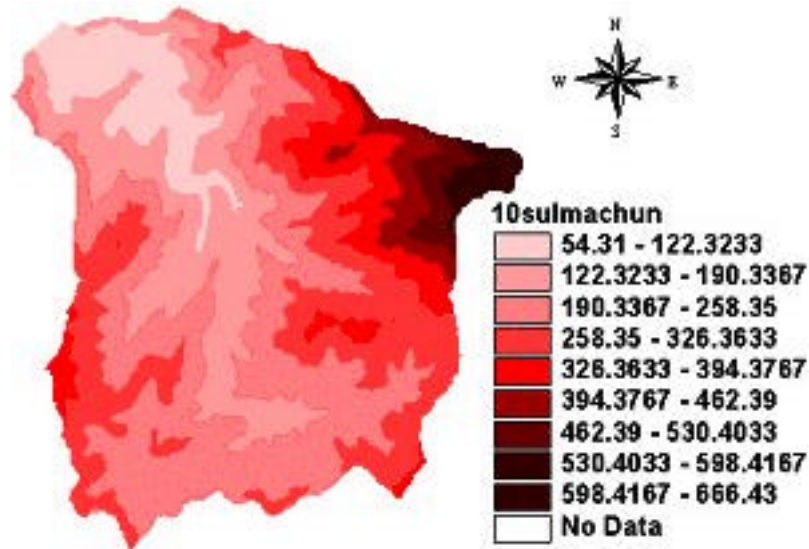


Figure 2. Digital elevation model (m) with 10 m pixel size of the Sulmachun watershed

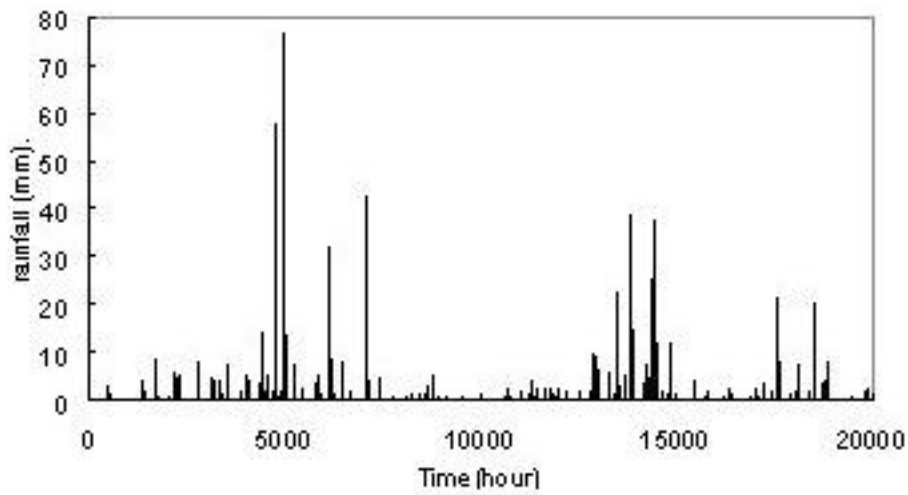
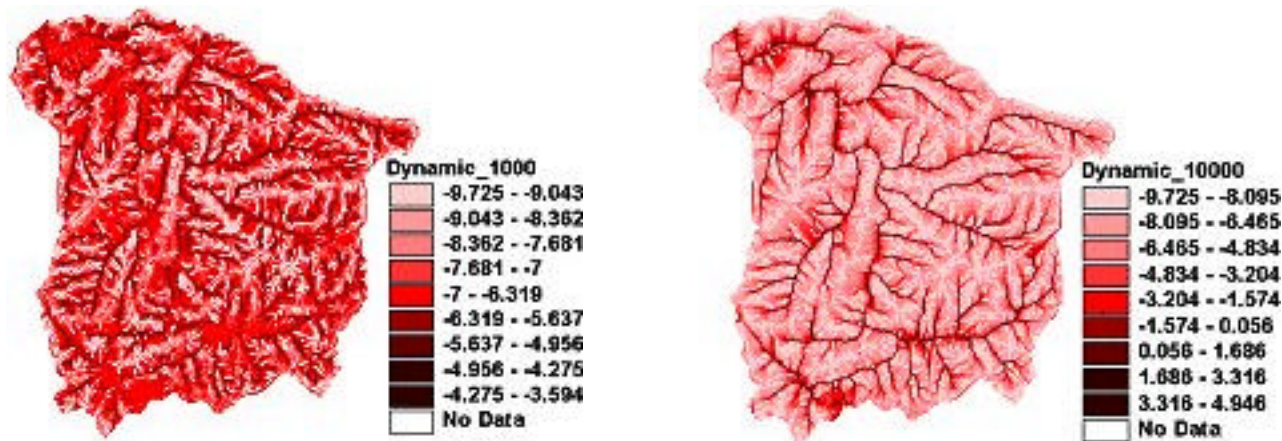


Figure 3. Rainfall of Sulmachun watershed from Jan. 6th of 1999 to April 18th 2001



(a) 1000 Hours (b) 10,000 Hours  
 Figure 4. Spatial distributions of dynamic wetness

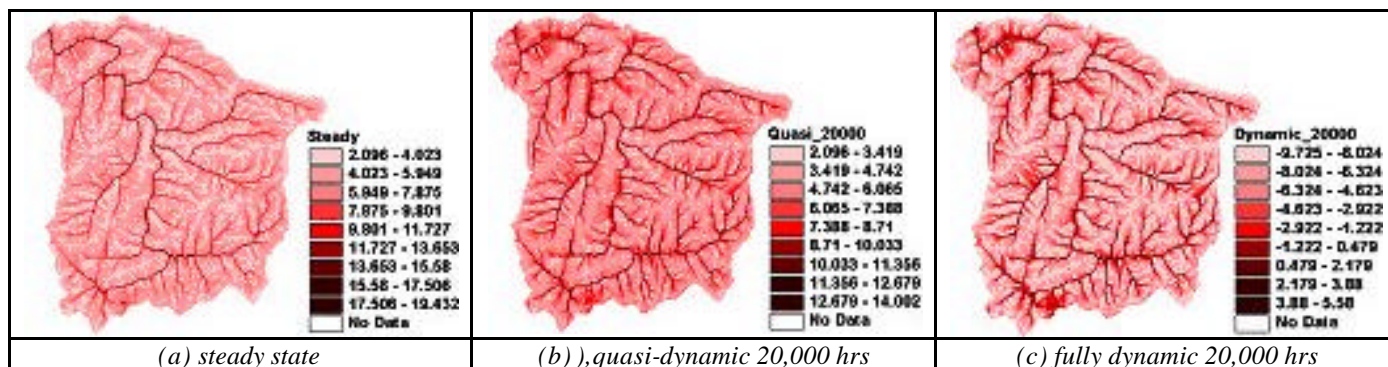


Figure 5. Wetness indices

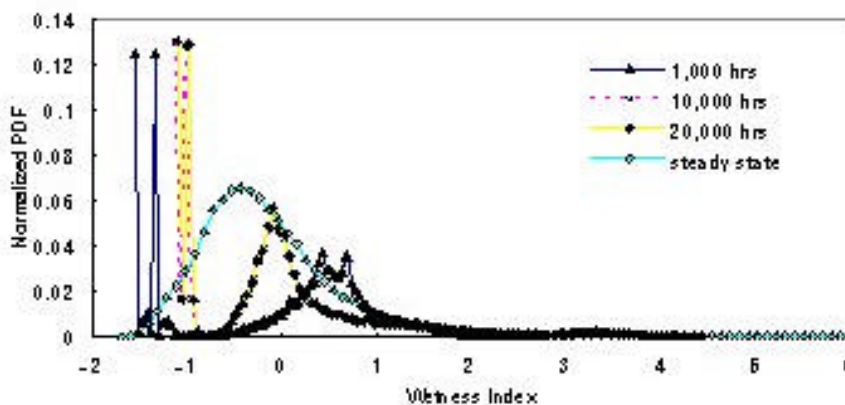


Figure 6. Normalized probability density functions of wetness indices

**CONCLUSIONS**

The dynamic wetness index was developed by integrating the convolution integral of rainfall with the single flow direction flow determination scheme. The spatial and temporal distribution of the dynamic topographic wetness index were presented and compared with the quasi-dynamic and steady wetness index. The organization patterns of wetness index can be observed over various drainage times. The impact of temporal heterogeneity of rainfall to the saturation distribution pattern can be evaluated by the DEM analysis of the flow determination. The dual distribution of the normalized PDF of the dynamic wetness index indicates the existence of a completely different saturation characteristic from that of the steady assumption results primarily in the diverging areas of the watershed. The normalized PDFs of the quasi-dynamic and the dynamic wetness indices show the existence of the threshold pixel size of the DEM which provides stability and consistency in the computation of saturation patterns with temporal variability of rainfall.

**ACKNOWLEDGEMENT**

This research was supported by a grant (2-1-1) from Sustainable Water Resources Research Center of 21st Century Frontier Research Program.



**REFERENCES**

Barling RD, Moore ID, Grayson RB.(1994). A quasi-dynamic wetness index for characterising the spatial distribution of zones of surface saturation and soil water content. *Wat. Res. Resear.*, **30**, 1029-1044

Beven KJ, Wood EF. (1983). Catchment geomorphology and the dynamics of runoff contributing areas. *J. of Hydro.*, **65**,139-158.

Kim S.H., Delleur J.W., (2001). Stochastic structures between quantity and quality reponses of rainfall-runoff at an upland agricultural watershed, *Wat. Sci. Tech.*, **44**(7), 91-104, (2001)

O'Callaghan, J. F., and D. M. Mark. (1984). The extraction of drainage networks from digital elevation data. *Computer Vision. Gra. Im. Proc.*, **28**, 323-344.

Perrone J., Madramootoo C.A. (1999). Sediment yield prediction using AGNPS, *J. Soil Wat. Cons.*, **54**(1), 415-419.

Quinn, P., K. Beven, P. Chevallier, and O. Planchon. (1991). The prediction of hillslope flow paths for distributed hydrological modeling using digital terrain models. *Hydro. Proc.* **5**, 59-79.

Torbert HA., Potter K.N., Hoffman D.W., Gerik T.J. (1999). Richardson C.W., Surface residue and soil moisture affect fertilizer loss in simulated runoff on a heavy clay soil. *Agr. J.* **91**(4), 606-612.

Vukovic M. and Soro A. (1992). Determination of hydraulic conductivity of porous media from grain-size composition, *Water Resources Publications*, 25-83.

Wallach R., Grigorin G., Rivlin J., (2001). A comprehensive mathematical model for transport of soil-dissolved chemicals by overland flow. *J. Hydro.* **247**(1-2), 85-99.

Western AW, Graysen R, Blöschl G, Willgoose G, McMahon TA. (1999) Observed spatial organization of soil moisture and its relation to terrain indices. *Wat. Res. Resear.* **35**, 797-810.

Wigmosta MS, Lettenmaier DP. (1999). A comparison of simplified methods for routing topographically driven subsurface flow. *Wat. Res. Resear.* **35**, 255-264.

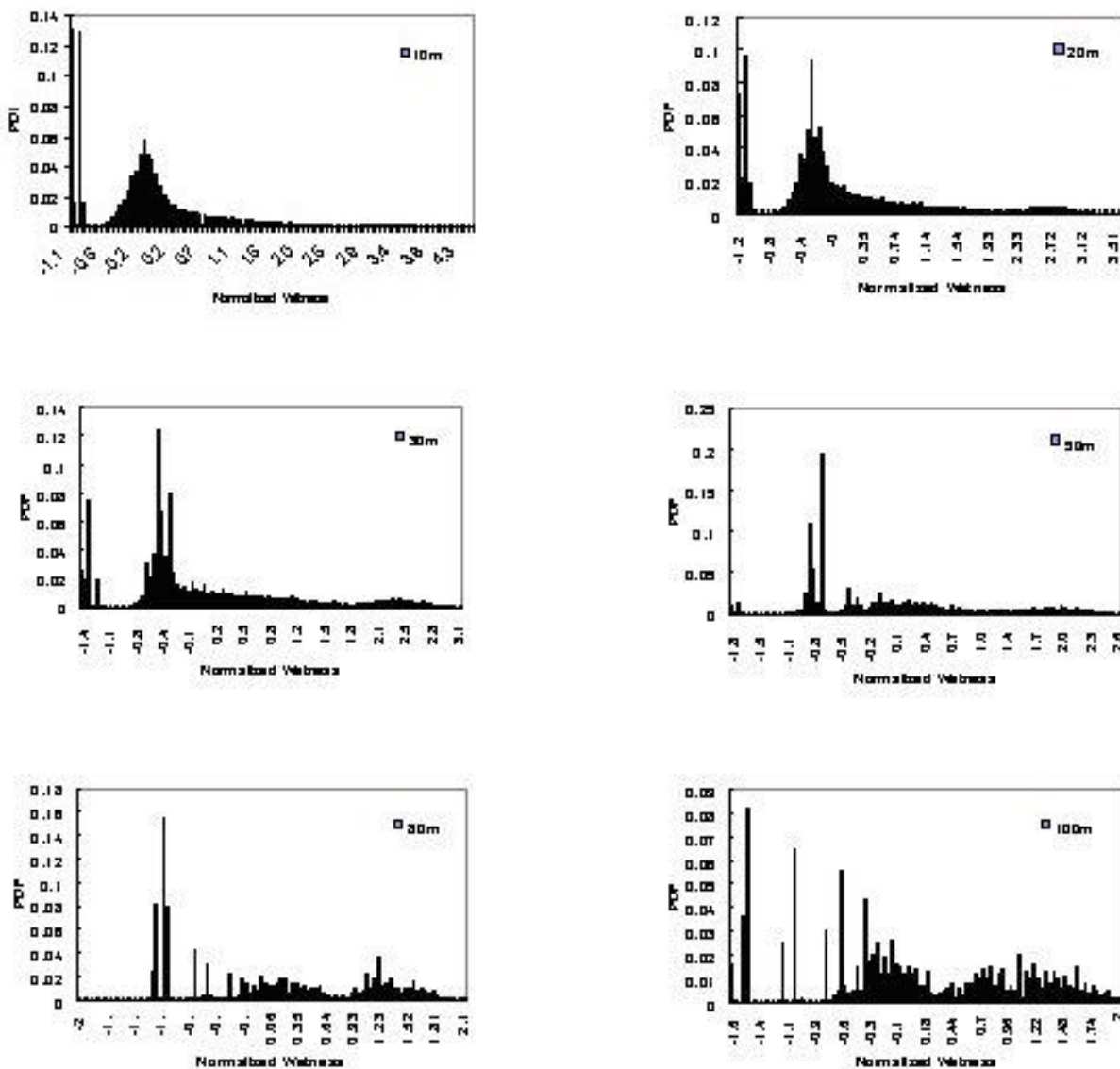


Figure 7. Normalized dynamic wetness indices of various resolutions (10, 20 30, 50, 80, 100 m)